

**INTERACTION BETWEEN TWO WEB SPANS
BECAUSE OF A MISALIGNED DOWNSTREAM ROLLER**

by

**J. J. Shelton
Oklahoma State University
USA**

ABSTRACT

Fourth order differential equations for two web spans are solved, with the required eight boundary conditions reflecting conditions at the upstream end of the first span, the downstream end of the second span (at the misaligned roller), and at the roller between the two spans, where slippage occurs. Required relationships between the moment and lateral force at the slipping roller are derived from analysis of distributed frictional vectors across the web, along with the auxiliary variable K_s , which is determined by the curvature and slope of the web at the intermediate roller. The solution of three equations with three unknowns is accomplished by iteration, then the three parameters are substituted into the solutions of the differential equations.

The patch of contact between the web and the intermediate roller is assumed to be rigid, as supported by many observations and photographs. The distributed loading on the intermediate roller is assumed to be uniform, but the effects of a nonuniform loading as imposed by a web wrapping the roller are examined and found to be little different from the effects of a uniform loading.

Besides identifying the conditions which lead to failure of a guide, interaction of spans is established as a potentially major source of erratic lateral behavior of a web, including a newly identified "jump" phenomenon. Another result includes identification of conditions which would cause a slack edge.

Because of the potentially severe problems of lateral behavior when interaction occurs, simple methods for prevention of interaction are recommended for installation of steering guides. Also, tolerances for parallelism of stationary rollers for avoidance of interaction are recommended.

The results of the analysis compared favorably with existing experimental data for the case of the web wrapping the slipping roller, even when the steering was great enough to cause a slack edge.

NOMENCLATURE

A	designation of pre-entering span of misaligned roller	ℓ	as a subscript, pertaining to the lateral direction
B	designation of entering span of misaligned roller	M	bending moment in the web
$C_{A1}, C_{A2} \dots C_{B3}, C_{B4}$	coefficients of differential equations, dependent upon L/W , ϵ , and E/G	M_r	moment on the web caused by circumferential slippage at the first roller upstream from a misaligned roller
c	as a subscript, pertaining to the circumferential direction	N	shear force normal to the elastic curve of the web
E	modulus of elasticity (Young's Modulus)	o	as a subscript, denotes a condition at the upstream roller
G	modulus of elasticity in shear	Q	resultant frictional forces
F	resultant force	q	distributed frictional forces
F_r	lateral force on the web caused by lateral slippage at the first roller upstream from a misaligned roller	T	total (resultant) web tension
f	distributed force	t	web thickness
I	moment of inertia of the web ($tW^3/12$)	V	velocity of web travel
K	a parameter, constant for a given operating condition ($\sqrt{T/EI}$ or $\sqrt{12\epsilon/W}$)	v	local velocity of slippage
K_s	ratio of lateral slippage velocity to circumferential slippage velocity for specific averages	W	web width
L	as a subscript, denotes a condition at the downstream roller	x	distance parallel to the original center line of the web
L	the length of a free span of a web	y	lateral web deflection from its original position
		ϵ	strain
		θ_r	angle of misalignment – radians
		θ_w	angle of wrap of the web – radians
		μ	coefficient of friction (sum of coefficients for a pair of nip rollers)
		σ	average tensile stress (T/tW)

INTRODUCTION

Shown in Figure 1 is the primary detrimental, sometimes catastrophic, result of upstream moment transfer, the amplification of error in a long pre-entering span with a short entering span of a steering guide or an improperly installed displacement guide. The web guide then appears to be correcting the upstream error within the limit of its stroke, whereas the guide is actually amplifying the upstream error, perhaps resulting in more overall error than that which would occur if the guide were eliminated or locked in its centered position.

Problems caused by the upstream transfer of moment are rarely identified because of the almost nonexistence of publicity of the problem, and because of the counterintuitive location of the cause and effect. Because of upstream transfer of moment, opposite in each half of the web, a bowed roller can cause wrinkling in its pre-entering span, sometimes in the form of a large, continuous foldover down the center of the web. Thus, a spreading device which appears to be working properly may have caused the very defect which it appears to be correcting or reducing.

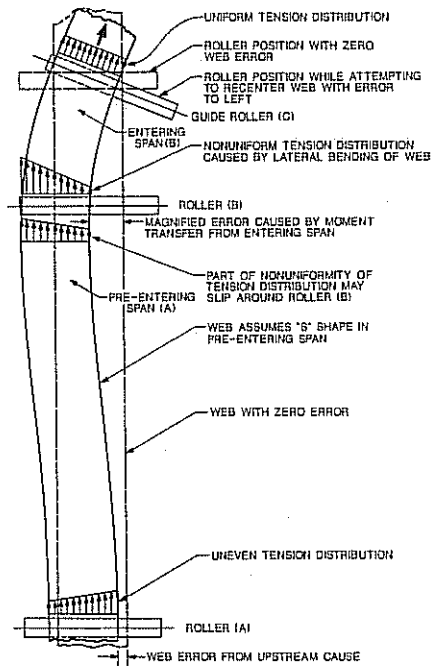


Figure 1 – Pre-Entering Span Steering Caused by Web Guide (Long Pre-Entering Span)

Besides the needed quantification of the effects of upstream transfer of moment caused by a web guide, this study should aid in understanding of sources of lateral disturbances in systems of stationary rollers in which one or several rollers are unintentionally misaligned. This knowledge may result in guidelines for proportioning span lengths during the initial design of process lines for reducing the effects of misalignment of rollers, or in pinpointing rollers which need special attention to cylindricity and alignment.

Figure 2(a) shows loading of the web on an unwrapped roller by means of a nip roller, or perhaps by the weight of a heavy web on a support roller with little wrap, so that the loading across the roller is uniform and unaffected by the tension and distribution of tension in the web. Figure 2(b) shows the more common case of a wrapped roller, where the total loading of the web on the roller

as well as the distribution of the loading depend on the tension and bending moment in the web. This paper shows that the simpler analysis is reasonably accurate when applied to a wrapped roller. The results could similarly be applied to a vacuum roller, where the loading caused by web tension is augmented by a vacuum from inside the contact patch.

The analyses of this paper are only for steady-state conditions, but the dynamic behavior is related to the time constants of the spans.

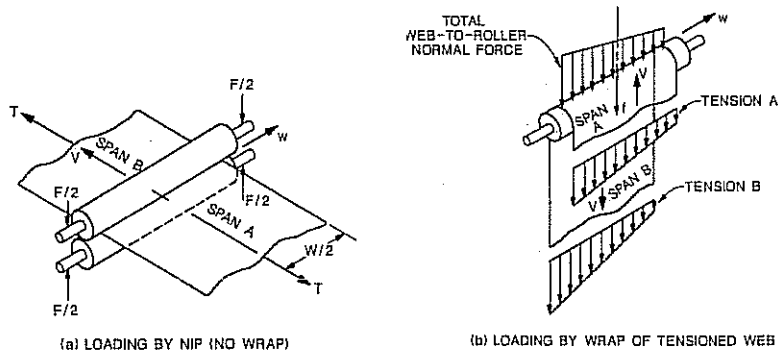


Figure 2 – Two Methods For Generating Traction Between Web and Roller

LATERAL FORCE AND MOMENT ON A WEB AT A SLIPPING ROLLER

Friction Characteristics and Frictional Force Vectors

Coulomb friction is assumed in this analysis, although web-to-roller friction may in some cases exhibit a higher breakaway friction than the sliding friction, and the sliding friction may be dependent on the relative velocity. Some plastic materials approach the Newtonian theory of liquids, wherein the friction force is proportional to the relative velocity, as well as being proportional to the loading. The assumption of Coulomb friction is justified by the fact that the coefficient of friction is never known precisely in web handling, as it varies with velocity, temperature, moisture, contamination, etc.

Based on the assumption of Coulomb friction, the frictional force on each differential area of the web is proportional to the pressure between the web and roller, and is in the direction opposite the direction of the resultant velocity of slippage. An example is shown in Figure 3 for the case of the unwrapped roller of Figure 2(a), and for the special operating condition wherein the circumferential velocity of slippage at the edges is equal to the lateral velocity of slippage across the web.

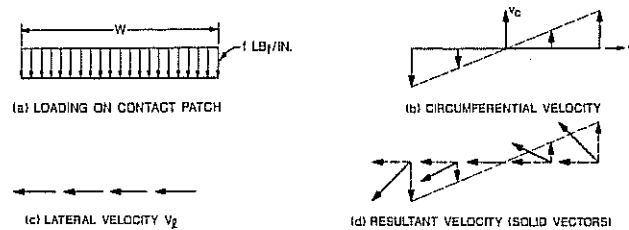


Figure 3 – Nip-Loaded Narrow Contact Patch With Circumferential and Lateral Velocities of Slippage Equal at Edges ($K_s = 1.0$)

For the case of the line contact of a set of nip rollers with no wrap, the magnitude is proportional to the constant distributed load (force per unit length) and the sum of the coefficients of friction between the web and each roller.

If an idler is wrapped by the web as in Figure 2(b), the pressure of the web on the roller at a given point is the local distributed tension (force per unit width) divided by the radius of the roller. Even if the web were initially straight as well as uniform across its width, the pressure in the contact patch would vary if a bending moment were present in the web upstream and/or downstream of the contact patch. Such bending moments are dependent on conditions upstream and downstream of the contact patch, as well as the frictional moment and lateral force if slippage occurs across the contact patch. In fact, all of these conditions then are interdependent, requiring simultaneous solution of differential equations of the tensioned beams between the rollers as well as equations of the effects of the frictional forces in the contact patch.

The following analysis neglects distortion within the contact patch. This assumption is believed to be realistic if the contact patch is narrow in comparison to the lengths of the adjacent spans. Figure 4 shows a bridle (as commonly used for transport of metal webs), for which the lengths of web within the contact patches are much greater than the length of span B. Misalignment of roller B is the subject of this

analysis (with the behavior of the wide contact patch approximated as a line of contact), whereas the Shelton thesis [1] and other analyses predict the results of misalignment of the complete bridle.

As in the usual application of beam theory, the exact local stress distribution is replaced by the equivalent moment and normal force, assumed to be applied at points, as justified by the Principle of Saint Venant. This principle states that, at points “distant” from the locality of application of loading, the results do not depend on the exact nature of the loading. The importance of the Principle of Saint Venant in this analysis lies in the fact that, even if the web is loaded by a nip with no wrap, the distributions of frictional forces across the web are nonlinear, even if tension distributions distant from a roller vary linearly, as shown in Figure 2(b).

Figure 2(b) shows the total web-to-roller normal force as a linear distribution of forces across the roller at the center of the angle of wrap. This loading is taken as the average of the loading corresponding to the tension distribution at the line of entering contact applied over one half of the angle of wrap, and the loading corresponding to the tension distribution at the line of exiting contact applied over the other half of the angle of wrap.

The assumption of a rigid web within the contact patch was formulated from observation of specific webs with slack edges. As sketched in Figure 5, the slackness of the entering span has been observed to extend to the misaligned roller, contrary to the slack-edge analysis by Shelton [2]. The downstream boundary condition in the latter analysis was assumed to be a moment of zero as proven in the Shelton thesis for the case of tautness throughout the entering span. The exiting span as sketched in Figure 5 has been observed to have neither slackness nor an uneven distribution of tension, a condition explained by sufficient rigidity of the cylindrical shell of the contact patch for prevention of the transfer of slackness or of an uneven distribution of tension across the roller. The taut exiting span further bolsters the contact patch against distortion. In contrast, if the web consisted of independent tapes, or strings as in tire cord fabric, and if slackness existed in a longitudinal element on one side of a roller, the element would have to be slack in the span across the contact patch.

Definition of Velocity Slippage Ratio K_s

The dependent variable K_s is introduced to facilitate analysis. If the loading on the contact patch is uniform as in Figure 3, the forward slippage rate at one edge is the same as the backward slippage rate at the other edge, and K_s can be defined as the ratio of the lateral slippage velocity divided by the circumferential slippage velocity at the edges. If the normal force of the web on the roller is nonuniform as in Figure 2(b), however, the circumferential slippage velocity is greater on the lightly loaded edge

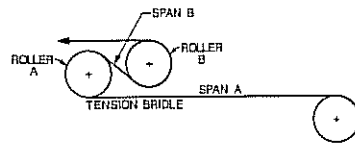


Figure 4 – Tension Bridle As Used For Metal Strip

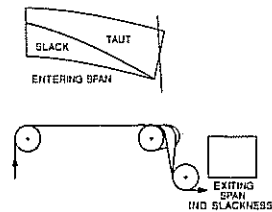


Figure 5 – Observed Slack Edge in Entering Span of Steering Guide

than on the heavily loaded edge. For this condition of nonuniform normal force along with the assumption of small friction losses, the slippage ratio K_s is defined as

$$K_s = \frac{2}{W} \frac{y'_{AVG}}{y''_{AVG}} \quad \{1\}$$

In equation (1), in the interest of practicality of solution, y'_{AVG} is used as $(y'_{AL} + y'_{BO})/2$ and y''_{AVG} is used as $(y''_{AL} + y''_{BO})/2$, so that equation (1) can be written as

$$K_s = \frac{2}{W} \frac{y'_{AL} + y'_{BO}}{y''_{AL} + y''_{BO}}, \quad \{2\}$$

where span A is upstream and span B is downstream from the roller being studied.

Frictional Forces within the Contact Patch

For Coulomb friction as modeled, the solid vectors of velocity in Figure 3(d) indicate the direction (opposite the velocity of slippage) but not the magnitude of the force vectors in the contact patch. The differential magnitude for this case of line contact with uniform loading is f force per unit length multiplied by the coefficient of friction and the differential length along the line of contact.

Figure 6 represents the first quantification of the qualitative insight from the mid-1960s: When friction is insufficient to prevent the transfer of moment from a downstream span to an upstream span, the velocity of circumferential slippage is low

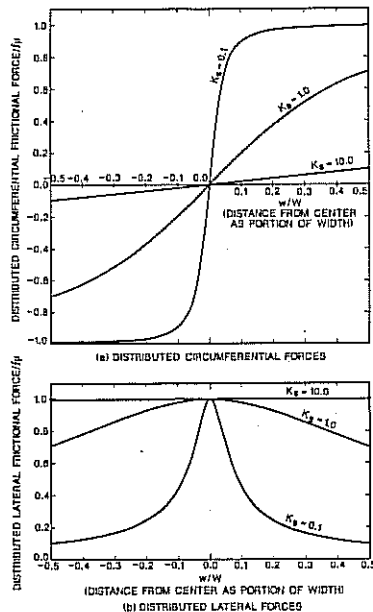


Figure 6 – Distributed Incremental Frictional Forces – Uniform Loading

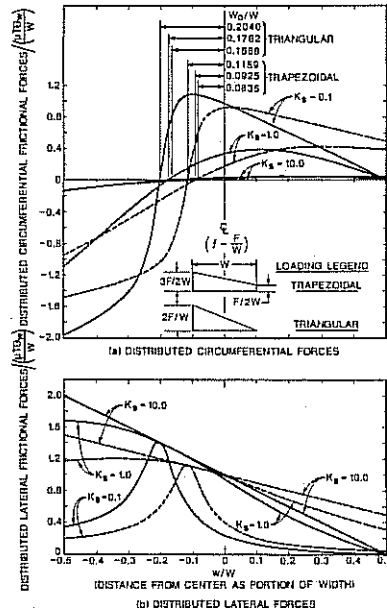


Figure 7 – Distributed Incremental Frictional Forces on Wrapped Roller

near the center of the web, perhaps allowing the lateral friction near the center to steer the web into a nearly perpendicular relationship with the roller. This study, however, found the relationship to be not truly perpendicular.

Analysis of the frictional forces within the contact patch of a wrapped roller was accomplished, as shown in Figure 7. Figure 8 compares the lateral force, the frictional moment and its total moment arm, and the forward and backward circumferential loading for uniform, trapezoidal (midway between triangular and uniform) and triangular loading.

These variables for the trapezoidal loading are very near those for uniform loading, and are reasonably near for triangular loading, even though the plots of distributed loading in Figures 6 and 7 are vastly different. For the nonuniform loads in Figure 8, F is equal to the total loading ($T\theta_w$). Figure 8 along with experimental results are considered to be justification for using the analysis of uniform loading for a wrapped roller. Analysis of the distributed forces of Figure 6 results in the relationships

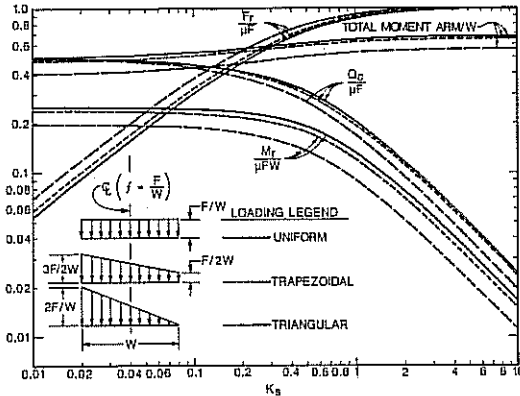


Figure 8 – Comparison of Nonuniform and Uniform Loading on Slipping Roller

$$\frac{F_r}{EtW\theta_r} = K_s \frac{\mu f}{Et\theta_r} \ln \frac{2 + \sqrt{1 + K_s^2}}{K_s} \quad \{3\}$$

and

$$\frac{M_r}{EtW^2\theta_r} = \frac{\mu f}{4Et\theta_r} \left[\sqrt{1 + K_s^2} \ln \frac{K_s}{2 + \sqrt{1 + K_s^2}} \right] \quad \{4\}$$

Condition of Borderline Interaction

The troublesome behavior of interacting spans can be avoided if the first roller upstream from a guide has friction sufficient to prevent the transfer of moment to the next upstream span. The maximum moment which a roller can resist without slippage is $f\mu W / 2$ multiplied by the moment arm of one-half the web width, or

$$M_r)_{\max} = f\mu W^2 / 4 . \quad \{5\}$$

Equation {5}, combined with the general relationship between the bending moment and the curvature along with the relationship between y''_{BO} and other parameters for a short span with a misaligned downstream roller (from Shelton [3]),

results in

$$\frac{\theta_r Et}{f\mu} < \frac{(E/G) + 6(L_B/W)^2}{4L_B/W}, \quad \{6\}$$

if L/W is less than 3.5, but greater than 0.25.

The maximum lateral force which a roller can exert on the web, if circumferential slippage has not occurred, is

$$F_r)_{\max} = f\mu W. \quad \{7\}$$

Equation {7}, combined with the general relationship between the lateral force and the third derivative of the elastic curve, along with the relationship between y'''_{BO} and other parameters for a short span with a misaligned roller (from Shelton [3]), results in

$$\frac{\theta_r Et}{f\mu} < \frac{E}{G} + 6\left(\frac{L_B}{W}\right)^2. \quad \{8\}$$

Equation {8} specifies avoidance of interaction of spans when L_B/W is less than 0.25.

For a long span ($L/W > 3.5$), equation {2.1.22} of the Shelton thesis [1] (with T/K expressed as $EtW^3K/12$) can be combined with moment equations to obtain:

$$\frac{\theta_r Et}{f\mu} < \frac{3}{KW} \frac{\cosh KL_B - 1}{\sinh KL_B}. \quad \{9\}$$

BOUNDARY CONDITIONS AND SOLUTIONS OF DIFFERENTIAL EQUATIONS

Strategy of Solution

The elastic curves of two interacting spans are discontinuous at the intermediate roller; therefore, different equations are required for the two spans. Fourth-order differential equations are to be solved; therefore, four boundary conditions are required for each span. Figure 9 shows eight boundary conditions which are applicable if L/W for each span is less than 3.5; however, M_r and F_r in two of the boundary-condition equations are initially unknown, and must be found from equations {2}, {3}, and {4}.

Equation {2} defines K_s in terms of derivatives of the elastic curves evaluated at the

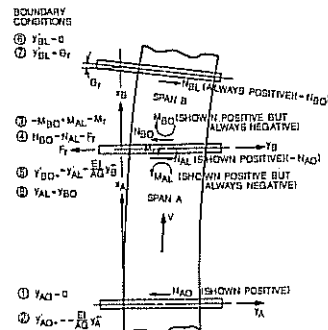


Figure 9 – Circumferential and Lateral Slippage Between Two Web Spans (Short-Span Theory)

intermediate roller. An iterative solution of these three independent equations for known values of web elasticity, dimensions of the web and the spans, operating conditions, and the parameter $\theta_r Et / f\mu$ determines K_s , from which M_r and F_r are determined. The two elastic curves and their derivatives can then be evaluated.

Solutions will be obtained for three combinations of span lengths, where a "short span" has L/W less than 3.5 and a "long span" has L/W greater than 3.5:

Both Spans Short. From Shelton [3], the differential equations for the two spans are

$$\frac{d^4 y_A}{dx_A^4} = 0 \quad \text{and} \quad \frac{d^4 y_B}{dx_B^4} = 0. \quad \{10\}$$

General nondimensionalized solutions are

$$\begin{aligned} \frac{y_A}{W\theta_r} &= \frac{C_{A1} W^2}{\theta_r} \left(\frac{x_A}{W}\right)^3 + \frac{C_{A2} W}{\theta_r} \left(\frac{x_A}{W}\right)^2 + \frac{C_{A3}}{\theta_r} \frac{x_A}{W} + \frac{C_{A4}}{W\theta_r}, \text{ and} \\ \frac{y_B}{W\theta_r} &= \frac{C_{B1} W^2}{\theta_r} \left(\frac{x_B}{W}\right)^3 + \frac{C_{B2} W}{\theta_r} \left(\frac{x_B}{W}\right)^2 + \frac{C_{B3}}{\theta_r} \frac{x_B}{W} + \frac{C_{B4}}{W\theta_r}. \end{aligned} \quad \{11\}$$

After substitution of derivatives of equations {11}, equation {2} becomes:

$$K_s = \frac{\frac{C_{A1} W^2}{\theta_r} \left[3 \left(\frac{L_A}{W}\right)^2 - \frac{1}{2} \frac{E}{G} \right] + \frac{C_{A2} W}{\theta_r} \left[2 \frac{L_A}{W} \right] + \frac{C_{B3}}{\theta_r}}{\frac{C_{A1} W^2}{\theta_r} \left[3 \frac{L_A}{W} \right] + \frac{C_{A2} W}{\theta_r} + \frac{C_{B2} W}{\theta_r}}. \quad \{12\}$$

The boundary conditions for two short spans are shown in Figure 9.

Both Spans Long. The differential equations for the two spans are

$$\frac{d^4 y_A}{dx_A^4} - K^2 \frac{d^2 y_A}{dx_A^2} = 0 \quad \text{and} \quad \frac{d^4 y_B}{dx_B^4} - K^2 \frac{d^2 y_B}{dx_B^2} = 0. \quad \{13\}$$

General nondimensionalized solutions are

$$\begin{aligned} \frac{y_A}{W\theta_r} &= \frac{C_{A1}}{W\theta_r} \sinh Kx_A + \frac{C_{A2}}{W\theta_r} \cosh Kx_A + \frac{C_{A3}}{\theta_r} \frac{x_A}{W} + \frac{C_{A4}}{W\theta_r}, \text{ and} \\ \frac{y_B}{W\theta_r} &= \frac{C_{B1}}{W\theta_r} \sinh Kx_B + \frac{C_{B2}}{W\theta_r} \cosh Kx_B + \frac{C_{B3}}{\theta_r} \frac{x_B}{W} + \frac{C_{B4}}{W\theta_r}. \end{aligned} \quad \{14\}$$

Three boundary conditions in Figure 9 must be modified to reflect the insignificance of shear deflections in long spans: (2) $y'_{A0} = 0$, (4) $F_r = -Ely''_{B0} + Ely''_{AL}$, and (5) $y'_{B0} = y'_{AL}$. Also, the notes on Figure 9 about normal forces are not applicable ($N_{AL} \neq N_{A0}$ and $N_{BL} \neq N_{B0}$ for long spans).

Substitution of derivatives of equations {14} into equation {2} results in

$$K_s = \frac{2}{(KW)^2} \frac{\frac{C_{A1}}{W\theta_r} KW \cosh KL_A + \frac{C_{A2}}{W\theta_r} KW \sinh KL_A + \frac{C_{A3}}{\theta_r} + \frac{C_{B1}}{W\theta_r} KW + \frac{C_{B3}}{\theta_r}}{\frac{C_{A1}}{W\theta_r} \sinh KL_A + \frac{C_{A2}}{W\theta_r} \cosh KL_A + \frac{C_{B2}}{W\theta_r}} \quad \{15\}$$

Comparison of Long-Span and Short-Span Theory. Figures 10 and 11 compare the long-span theory and the short-span theory for L_A / W and L_B / W of 3.5, higher than the value of 2.0 for which the short-span theory is generally precise and lower than the value of 5.0 or so for which the long-span theory is precise. The graphs are plotted for E/G of 2.7 for the short-span theory and ϵ of 0.001 for the long-span theory. Curves with ϵ of 0.0001 were calculated, but could not be distinguished from the dashed curves for ϵ of 0.001. Thus, there appears to be no need for analysis of two spans of intermediate length (L / W of 2.0 to 5.0) using the more complicated "Timoshenko beam" theory.

Long Pre-Entering Span and Short Entering Span. This analysis applies the "Euler beam" theory to the long span and the Shelton short-span theory [3] to the entering span. Based on Figure 10, L/W of the entering span can be as great as 3.5 and L/W of the pre-entering span as small as 3.5 for satisfactory application of this theory.

The boundary conditions shown in Figure 9 apply to this analysis except for the second condition, which is changed to reflect the negligible angle caused by shear in the upstream span; specifically, (2) $y'_{A0} = 0$. Also, the note that $N_{AL} = N_{A0}$ is not applicable.

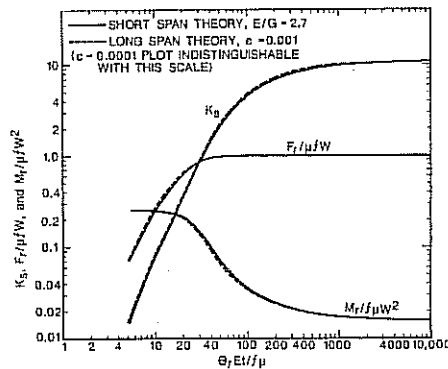


Figure 10 – Comparison of Short Span and Long Span Theory
 $L_A / W = 3.5, L_B / W = 3.5$

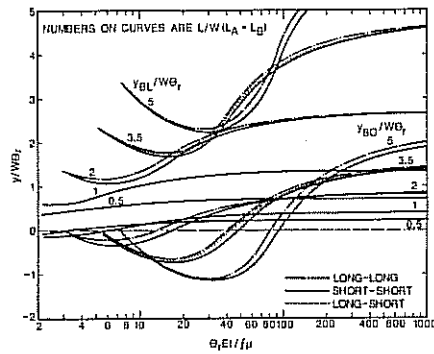


Figure 11 – Comparisons of Theory – Displacements of Equal Spans
 $\epsilon = 0.001 \quad E / G = 2.7$

The differential equations are:

$$\frac{d^4 y_A}{dx_A^4} - K^2 \frac{d^3 y_A}{dx_A^3} = 0 \quad \text{and} \quad \frac{d^4 y_B}{dx_B^4} = 0. \quad \{16\}$$

General nondimensionalized solutions are

$$\begin{aligned} \frac{y_A}{W\theta_r} &= \frac{C_{A1}}{W\theta_r} \sinh Kx_A + \frac{C_{A2}}{W\theta_r} \cosh Kx_A + \frac{C_{A3}}{\theta_r} \left(\frac{x_A}{W} \right) + \frac{C_{A4}}{W\theta_r}, \text{ and} \\ \frac{y_B}{W\theta_r} &= \frac{C_{B1} W^2}{\theta_r} \left(\frac{x_B}{W} \right)^3 + \frac{C_{B2} W}{\theta_r} \left(\frac{x_B}{W} \right)^2 + \frac{C_{B3} x_B}{\theta_r W} + \frac{C_{B4}}{W\theta_r}. \end{aligned} \quad \{17\}$$

The nondimensional version of K_s for this combination of span lengths is

$$K_s = 2 \frac{\frac{C_{A1}}{W\theta_r} KW \cosh KL_A + \frac{C_{A2}}{W\theta_r} KW \sinh KL_A + \frac{C_{A3}}{\theta_r} + \frac{C_{B3}}{\theta_r}}{\frac{C_{A1}}{W\theta_r} (KW)^2 \sinh KL_A + \frac{C_{A2}}{W\theta_r} (KW)^2 \cosh KL_A + 2 \frac{C_{B2} W}{\theta_r}}. \quad \{18\}$$

Solution and Graphs of Results

Determination of the secondary variables K_s , $F_r / EtW\theta_r$, and $M_r / EtW^2\theta_r$ is an intermediate step in finding the lateral position, slope, moment, and normal force, along with related conditions (such as borderline slackness or potential wrinkling). For values of $\theta_r Et / f\mu$ wherein interaction occurs, as specified by equation {6}, {8}, or {9}, the secondary variables are single-valued and have no maximum or minimum values, but flatten out at high values of $\theta_r Et / f\mu$. Iterative solutions were therefore routine, consisting of a guess of K_s , then solution of the three equations for K_s . If the calculated value of K_s was higher than the assumed value, the assumed value had to be raised; if the calculated value was lower, including a physically meaningless negative value, the new assumption of K_s had to be lowered. For values of $\theta_r Et / f\mu$ greater than a certain value for a certain set of conditions, the numerical method converged by simple substitution of the calculated value of K_s for the new assumption; however, some calculations at low values of $\theta_r Et / f\mu$ required a digit-by-digit search for K_s several decimal places beyond the six significant digits used for final solutions.

Graphs similar to Figure 10 of the secondary variables were found to be disappointing in providing insight into final behavior. Many graphs (similar to Figure 11) of the variables of primary interest (lateral displacements, angle at the slipping roller, moments in the web, and lateral forces in the web) were then plotted for a large range of L/W values.

Final Results of Analysis. In Figure 11 and subsequent graphs, ease of comprehension is sacrificed in favor of compactness of documentation of the

graphical results for the case of a steering guide (variable θ_r) by using θ_r in both the independent and dependent variables. If interaction of spans did not occur, the displacement at a steering guide, y_{BL} , would be approximately proportional to θ_r ; hence, a horizontal zone in the $y/W\theta_r$ curve indicates that the displacement is there approximately proportional to θ_r , while a negative slope represents decreasing effectiveness of the guide, and a positive slope represents increasing sensitivity of lateral response to the guide. Figure 11 shows amplification of error as indicated by negative values of y_{BO} for equal-length spans with L/W of 2.0 or greater. A web guide cannot operate if $y_{BL}/W\theta_r$ is negative for any value of $\theta_r Et/f\mu$ which it may encounter, a common condition when L_A is somewhat greater than L_B . The correction may be inadequate if $y_{BL}/W\theta_r$ is small.

The nondimensionalizing factor $W/2\theta_r$ is used for an easy check of tautness. The web is taut across its width if

$$|y''W/2\theta_r| < \varepsilon/\theta_r. \quad \{19\}$$

The nondimensionalizing factor $W^2/12\theta_r$ is used for easy conversion between calculations and experimental measurement of lateral forces:

$$y'''W^2/12\theta_r = -(N/T)(\varepsilon/\theta_r), \quad \{20\}$$

where the sign conventions of the Shelton thesis [1] are used. It should be noted, however, that measurement of the lateral force from a roller is not generally the normal force in the web; further, a free body diagram of three or more rollers can be erroneous if the transport of shear forces across rollers is overlooked.

In addition to Figure 11, other results of analysis of two interacting spans of equal lengths with strain of 0.001, are shown in Figures 12 through 16. The negative slopes for wide ranges of $\theta_r Et/f\mu$ in Figures 11 and 12 indicate that a web guide operating

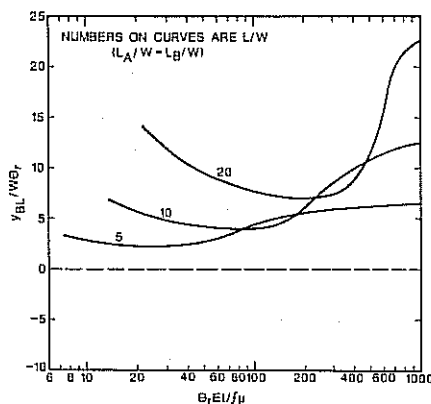


Figure 12 – Displacement at Misaligned Roller – Equal Spans $\varepsilon = 0.001$

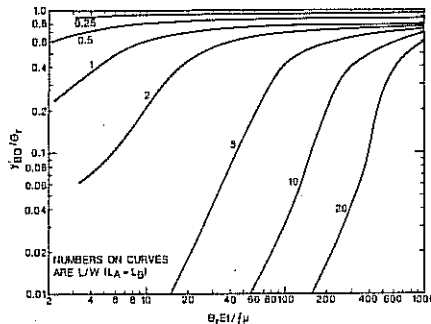


Figure 13 – Ratio of Slopes – Equal Spans $\varepsilon = 0.001$ $E/G = 2.7$

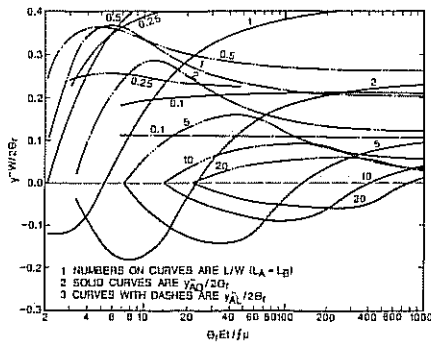


Figure 14 - Curvature - Equal Spans
 $\epsilon = 0.001$ $E/G = 2.7$

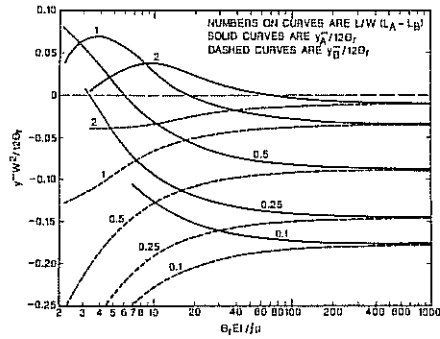


Figure 15 - Lateral Force Function - Equal Short Spans
 $E/G = 2.7$

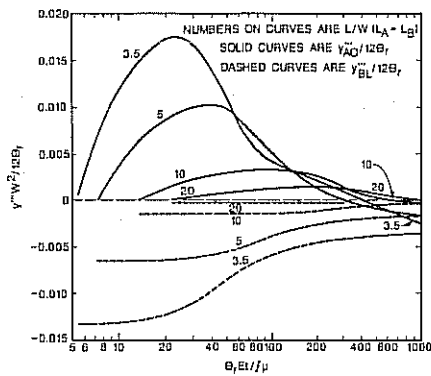


Figure 16 - Lateral Force Function - Equal Long Spans
 $\epsilon = 0.001$ $E/G = 2.7$

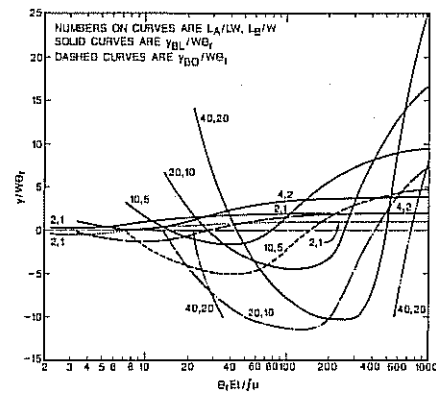


Figure 17 - Lateral Displacement - 2:1 Spans
 $\epsilon = 0.001$ $E/G = 2.7$

at such combinations of conditions would be handicapped by interaction. As interaction of two equal-length spans has not commonly been expected to cause a guiding problem, this result illustrates the need for analysis over the entire potential operating range of $\theta_r Et / f \mu$, or a need for prevention of interaction.

Figure 13 shows that the angle of the web at the slipping roller is less than the angle of misalignment, but greater than zero, as previously believed because of the inability to observe the usual small angle.

Figure 14 shows curvature at both ends of the pre-entering span, allowing a quick check of slackness by inequality {19}.

Figures 15 and 16 show the lateral force function, which can be converted to the lateral shear force in the web by equation {20}

Figure 17, for a strain of 0.001, agrees with many observations over the past forty years, that a pre-entering span twice as long as the entering span (or longer) commonly causes complete failure of a steering guide. Figure 18 shows the same result at a strain of 0.0001, a value more representative of conditions of handling metal strip.

Tables 1 and 2 show examples of calculations for equal-length spans and 2:1 spans, respectively. The first column for each case is the condition of borderline interaction. Line 2 is the lateral displacement compared to the lateral displacement for the non-slipping condition. A value other than unity for $y_{BL} / y_{BL,ns}$ identifies a lateral jump, as does a nonzero value of $y_{BO} / W\theta_r$, $y_{AO}'' W / 2\theta_r$, $y_{AL}'' W / 2\theta_r$, $y_{AO}''' W^2 / 12\theta_r$, and $y_{AL}''' W^2 / 12\theta_r$. An asterisk or an obelisk identifies interaction as being triggered by circumferential or lateral slippage, respectively.

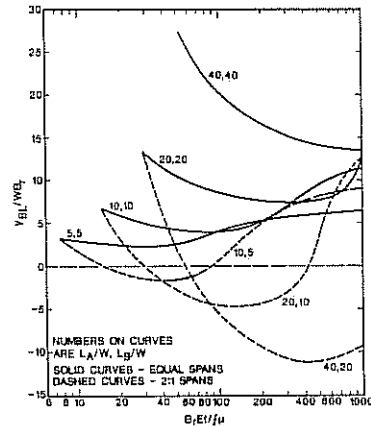


Figure 18 – Displacement at Misaligned Roller – Equal and 2:1 Spans $\epsilon = 0.0001$

Line	Variable	Case A: L_1/W and $L_2/W = 20$				Case B: L_1/W and $L_2/W = 10$			
		$\theta_r E/\mu$	30	100	300	13.66*	30	100	300
2	$y_{BL} / y_{BL,ns}$	1.00	0.839	0.542	0.518	1.00	0.717	0.595	1.27
3	$y_{BL} / W\theta_r$	14.2	12.0	7.72	7.37	6.84	4.87	4.05	8.62
4	$y_{BO} / W\theta_r$	0	-2.29	-6.55	-7.11	0	-1.93	-2.85	0.550
5	y_{BO} / θ_r	1.59(10) ⁻⁴	4.18(10) ⁻⁴ *	4.66(10) ⁻³	0.0420	0.00317	0.00293	0.0305	0.397
6	$y_{AO}'' W / 2\theta_r$	0	-0.0185	-0.0532	-0.0594	0	-0.0594	-0.0901	-0.0221
7	$y_{AL}'' W / 2\theta_r$	0	0.0186	0.0535	0.0623	0	0.0597	0.0934	0.0657
8	$y_{AO}''' W^2 / 12\theta_r$	0.0686	0.0685	0.0682	0.0657	0.110	0.110	0.107	0.0662
9	$y_{AL}''' W^2 / 12\theta_r$	0	4.24(10) ⁻⁴ *	0.00122	0.00137	0	0.00218	0.00334	0.00141
10	$y_{AL}''' W^2 / 12\theta_r$	0	4.24(10) ⁻⁴ *	0.00122	0.00141	0	0.00218	0.00337	0.00181
11	$y_{AL}''' W^2 / 12\theta_r$	-2.83(10) ⁻⁴ *	-2.83(10) ⁻⁴ *	-2.82(10) ⁻³	-2.72(10) ⁻⁴	-0.00151	-0.00151	-0.00146	-9.19(10) ⁻⁴

Line	Variable	Case C: L_1/W and $L_2/W = 5$				Case D: L_1/W and $L_2/W = 2$			
		$\theta_r E/\mu$	30	100	300	3.3375*	30	100	300
2	$y_{BL} / y_{BL,ns}$	1.00	0.689	1.32	1.79	0.913	1.46	1.78	1.87
3	$y_{BL} / W\theta_r$	3.36	2.31	4.41	6.00	1.28	2.05	2.49	2.62
4	$y_{BO} / W\theta_r$	0	-1.11	0.388	1.58	-0.0962	0.350	0.693	0.792
5	y_{BO} / θ_r	0.00107	0.0424	0.409	0.648	0.0618	0.546	0.699	0.742
6	$y_{AO}'' W / 2\theta_r$	0	-0.142	-0.0345	0.0611	-0.0370	0.0519	0.180	0.218
7	$y_{AL}'' W / 2\theta_r$	0	0.151	0.118	0.0717	0.0218	0.214	0.149	0.129
8	$y_{AO}''' W^2 / 12\theta_r$	0.205	0.196	0.121	0.0721	0.469	0.227	0.151	0.129
9	$y_{AL}''' W^2 / 12\theta_r$	0	0.0100	0.00502	3.89(10) ⁻³	0.00490	0.0135	-0.00264	-0.00744
10	$y_{AL}''' W^2 / 12\theta_r$	0	0.0101	0.00543	6.87(10) ⁻⁴	0.00490	0.0135	-0.00264	-0.00744
11	$y_{AL}''' W^2 / 12\theta_r$	-0.00650	-0.00623	-0.00384	-0.00239	-0.0391	-0.0189	-0.0126	-0.0108

Line	Variable	Case E: L_1/W and $L_2/W = 0.5$				Case F: L_1/W and $L_2/W = 0.1$			
		$\theta_r E/\mu$	30	100	300	2.76†	30	100	300
2	$y_{BL} / y_{BL,ns}$	0.784	1.53	1.58	1.60	1.01	1.46	1.49	1.50
3	$y_{BL} / W\theta_r$	0.345	0.674	0.696	0.703	0.109	0.147	0.148	0.149
4	$y_{BO} / W\theta_r$	-0.0895	0.199	0.219	0.225	0.01(10) ⁻⁴	0.0451	0.0483	0.0492
5	y_{BO} / θ_r	0.608	0.849	0.863	0.867	0.979	0.989	0.989	0.989
6	$y_{AO}'' W / 2\theta_r$	0	0.495	0.517	0.523	0.102	0.207	0.211	0.212
7	$y_{AL}'' W / 2\theta_r$	0.242	0.289	0.271	0.266	0.102	0.111	0.108	0.107
8	$y_{AO}''' W^2 / 12\theta_r$	0.785	0.302	0.275	0.267	0.214	0.116	0.109	0.107
9	$y_{AL}''' W^2 / 12\theta_r$	0.0811	-0.0684	-0.0819	-0.0858	0.02	-0.161	-0.172	-0.176
10	$y_{AL}''' W^2 / 12\theta_r$	0.0811	-0.0684	-0.0819	-0.0858	0.02	-0.161	-0.172	-0.176
11	$y_{AL}''' W^2 / 12\theta_r$	-0.262	-0.101	-0.0916	-0.0890	-0.356	-0.194	-0.182	-0.179

*Borderline circumferential slippage
†Borderline lateral slippage

Table 1. Interaction of Equal-Length Spans
 $\epsilon = 0.001$ (long spans) $E/G = 2.7$ (short spans)

Line	Variable	Case G: $L_A/W=40$ and $L_n/W=20$				Case H: $L_A/W=20$ and $L_n/W=10$			
		21.88*	30	100	300	13.66*	30	100	300
1	$\theta_r Et / f\mu$								
2	$y_{BL} / y_{BL,0}$	1	-0.0814	-0.655	0.476	1	-0.0814	-0.655	0.476
3	$y_{BL} / W\theta_r$	6.80	-0.553	-4.45	3.24	6.80	-0.553	-4.45	3.24
4	$y_{BO} / W\theta_r$	0	-7.70	-22.1	-25.0	0	-7.36	-11.3	-4.59
5	y_{BO} / θ_r	$1.59(10)^{-4}$	$3.95(10)^{-4}$	0.00409	0.0324	$3.23(10)^{-4}$	0.00228	0.0199	0.320
6	$y_{AO}^* W / 2\theta_r$	0	-0.0185	-0.0533	-0.0607	0	-0.0595	-0.0923	-0.0519
7	$y_{AL}^* W / 2\theta_r$	0	0.0186	0.0535	0.0626	0	0.0597	0.0937	0.0739
8	$y_{BO}^* W / 2\theta_r$	0.0686	0.0685	0.0683	0.0663	0.110	0.110	0.108	0.0747
9	$y_{AO}^* W^2 / 12\theta_r$	0	$3.47(10)^{-4}$	$9.97(10)^{-4}$	0.00114	0	0.00136	0.00212	0.00128
10	$y_{AL}^* W^2 / 12\theta_r$	0	$3.47(10)^{-4}$	0.00100	0.00117	0	0.00136	0.00214	0.00160
11	$y_{BO}^* W^2 / 12\theta_r$	$-2.83(10)^{-4}$	$-2.83(10)^{-4}$	$-2.82(10)^{-4}$	$-2.74(10)^{-4}$	-0.00151	-0.00151	-0.00148	-0.00103

Line	Variable	Case I: $L_A/W=10$ and $L_n/W=5$				Case J: $L_A/W=4$ and $L_n/W=2$			
		7.318*	30	100	300	3.3375*	30	100	300
1	$\theta_r Et / f\mu$								
2	$y_{BL} / y_{BL,0}$	1	-0.418	0.452	2.20	0.813	1.33	2.38	2.70
3	$y_{BL} / W\theta_r$	3.36	-1.40	1.52	7.36	1.14	1.86	3.34	3.78
4	$y_{BO} / W\theta_r$	0	-4.79	-2.35	2.84	-0.235	0.162	1.48	1.87
5	y_{BO} / θ_r	0.00107	0.0259	0.312	0.706	0.0611	0.541	0.787	0.857
6	$y_{AO}^* W / 2\theta_r$	0	-0.149	-0.103	0.0177	-0.0331	-0.0915	0.0885	0.143
7	$y_{AL}^* W / 2\theta_r$	0	0.152	0.137	0.0599	0.0218	0.216	0.105	0.0710
8	$y_{BO}^* W / 2\theta_r$	0.205	0.200	0.141	0.0602	0.469	0.230	0.107	0.0713
9	$y_{AO}^* W^2 / 12\theta_r$	0	0.00550	0.00422	$4.20(10)^{-4}$	0.00235	0.0128	$3.25(10)^{-4}$	-0.00345
10	$y_{AL}^* W^2 / 12\theta_r$	0	0.00552	0.00454	0.00113	0.00231	0.0133	0.00109	-0.00261
11	$y_{BO}^* W^2 / 12\theta_r$	-0.00650	-0.00633	-0.00447	-0.00191	-0.0391	-0.0191	-0.00888	-0.00594

Line	Variable	Case K: $L_A/W=1$ and $L_n/W=0.5$				Case L: $L_A/W=0.2$ and $L_n/W=0.1$			
		2.100*	30	100	300	2.76†	30	100	300
1	$\theta_r Et / f\mu$								
2	$y_{BL} / y_{BL,0}$	0.484	2.09	2.22	2.25	1.02	1.92	1.99	2.01
3	$y_{BL} / W\theta_r$	0.213	0.923	0.977	0.992	0.101	0.191	0.197	0.199
4	$y_{BO} / W\theta_r$	-0.220	0.440	0.491	0.506	0.00154	0.0911	0.0976	0.0994
5	y_{BO} / θ_r	0.602	0.897	0.914	0.918	0.979	0.989	0.990	0.990
6	$y_{AO}^* W / 2\theta_r$	-0.172	0.415	0.458	0.470	0.0965	0.289	0.299	0.302
7	$y_{AL}^* W / 2\theta_r$	0.243	0.199	0.171	0.163	0.102	0.106	0.103	0.102
8	$y_{BO}^* W / 2\theta_r$	0.797	0.207	0.173	0.164	0.211	0.111	0.104	0.102
9	$y_{AO}^* W^2 / 12\theta_r$	0.0692	-0.0360	-0.0478	-0.0512	0.00443	-0.152	-0.163	-0.167
10	$y_{AL}^* W^2 / 12\theta_r$	0.0692	-0.0360	-0.0478	-0.0512	0.00443	-0.152	-0.163	-0.167
11	$y_{BO}^* W^2 / 12\theta_r$	-0.0266	-0.0690	-0.0577	-0.0545	-0.352	-0.185	-0.173	-0.170

*Borderline circumferential slippage
†Borderline lateral slippage

Table 2. Interaction of 2:1 Spans
 $\epsilon = 0.001$ (long spans) $E/G = 2.7$ (short spans)

Lateral "Jump"

A phenomenon never previously observed or suspected, as far as is known, is the occurrence of two states of web behavior (lateral position, slope, moment, and lateral force) at the condition of borderline interaction (inequality signs changed to equalities in {6}, {8}, or {9}). The values of the dependent variables depend on whether $\theta_r Et / f\mu$ is increasing or decreasing as the borderline condition is approached. This phenomenon is called a "jump", even though it does not occur instantaneously, but is limited in time by the time constants of the spans upstream and downstream from the slipping roller. It occurs regardless of the characteristics of the friction, although it might be mistaken for a stick-slip phenomenon, and probably has been attributed to a sudden change in camber.

The magnitude of lateral jump is small if L_A / L_B is less than 0.25 or greater than 3.0 or so, unless the ratio L_A / L_B is large, as shown in Figures 19 and 20. The direction of lateral jump is opposite the direction of steering at the misaligned roller in

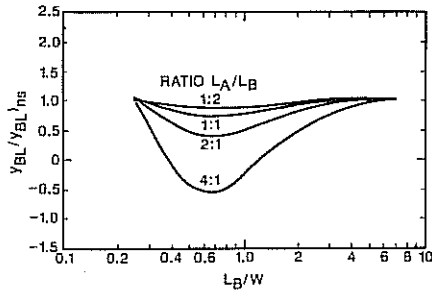


Figure 19 – “Jump” at Borderline Interaction Compared to Non-interactive Position

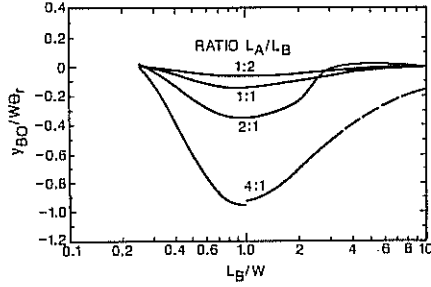


Figure 20 – “Jump” at Borderline Interaction

the absence of interaction when L_B/W is greater than 0.25, but is in the same direction as steering for smaller values of L_B/W . The magnitude of lateral jump when L_B/W is less than 0.25 was too small to plot as discrete curves in Figures 19 and 20. These figures show values of lateral jump great enough to cripple many web processes, especially if the ratio L_A/L_B is large and L_B/W is between 0.3 and 3.0.

EXPERIMENTAL VERIFICATION

Figure 21 compares the theory of this paper with tests reported by Good [4]. Test measurements were of lateral position of the web and lateral reactions of rollers. The agreement between the theory and tests is good, even for conditions of a slack edge, as shown with shaded data symbols. Please note that the frictional forces were generated by wrapping the roller with the web (90 degrees), as justified up to the condition of slackness of an edge by Figure 8.

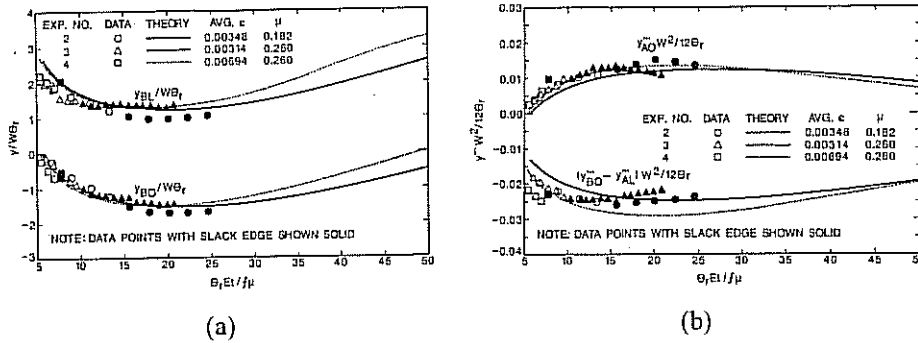


Figure 21 – Comparison of Theory and Experiments

$E/G = 2.7$ (Assumed)
 $W = 152.4$ mm
 $\theta_w = \pi/2$ radians

$t = 0.0356$ mm
 $E = 3.8$ GPa
 $L_A/W = 5.33, L_B/W = 4.0$

AVOIDANCE OF INTERACTION

Incentives for Avoidance of Interaction. The analysis of this report may explain many previously mysterious aspects of web handling, and thereby lay the foundation for design of process machinery which reduces the erratic lateral behavior of a web. The lateral position, as well as internal moments and shear forces, have been shown to be highly variable functions of the interaction variable $\theta_r Et / f \mu$. Hence, edge damage from excessive wander of the web, excessive stress caused by the moment, and wrinkling caused by the shear stresses may result from interaction.

The lateral jump which occurs at the onset of interaction over a wide range of parameters may detrimentally affect processes such as coating, printing, and slitting, if a web guide is not or cannot be located for correction of the lateral jump error.

If the entering span of a steering guide is preceded by a longer pre-entering span, complete failure of the web guide may occur because of positive feedback created by the interaction. If the guide is successful in correcting the interaction-induced error, the web is more likely to wrinkle or tear because of the increased shear and bending stresses caused by interaction.

Because of the multitude of problems caused by the interaction of spans, avoidance of interaction is examined in the following article.

Elimination of Interaction by Design of Processing Lines. Besides the ratios of span lengths, the primary independent variable established in this study is $\theta_r Et / f \mu$. Other variables of significant importance are strain for long spans and E/G for short spans. Variations of the latter, however, are not of major importance for webs which do not vary greatly from isotropy. This study established justification for neglecting the manner of application of the distributed force f , whether by a nip roller, vacuum roller, by wrap of the roller by the tensioned web, or by a combination of methods of generating the distributed force.

Inequalities {6}, {8}, and {9} for prevention of interaction indicate the need for a low value of the interaction variable $\theta_r Et / f \mu$. The variables E and t cannot be changed at the discretion of the process engineer, leaving the possibilities of decreasing θ_r and increasing f and μ for changing a condition of interaction to one of isolation of spans.

Figure 22 shows the maximum value of $\theta_r Et / f \mu$ as a function of L_B / W for avoidance of interaction as specified by inequalities {6}, {8}, and {9}, for a wide range of values of E/G and ϵ .

The most common source of the distributed loading f is the tension in the web along with wrap of a roller. A wrapped roller is so common and

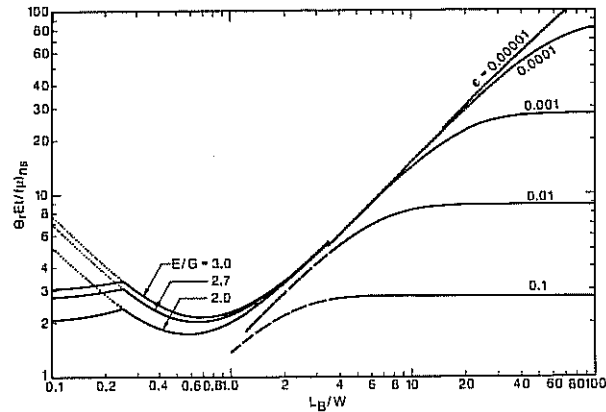


Figure 22 – Prevention of Interaction (Equations {6}, {8}, and {9})

the angle of wrap θ_w is usually so easily increased that simplification of the interaction variable $\theta_r Et / f\mu$ for this special case is justified. The simplification results from substitution of the simple relationships $f = (T/W)\theta_w$, where θ_w is in radians, and $\varepsilon = T/EtW$. The inequalities resulting from substitution into inequalities {6}, {8}, and {9} are

$$\frac{\theta_r}{\mu\theta_w} < \frac{\varepsilon}{4(L_B/W)} \left[\frac{E}{G} + 6 \left(\frac{L_B}{W} \right)^2 \right] \quad \{21\}$$

for $0.25 < (L_B/W) < 3.5$,

$$\frac{\theta_r}{\mu\theta_w} < \frac{\sqrt{3\varepsilon} \cosh KL_B - 1}{2 \sinh KL_B} \quad \{22\}$$

for $(L_B/W) > 3.5$, and

$$\frac{\theta_r}{\mu\theta_w} < \varepsilon \left[\frac{E}{G} + 6 \left(\frac{L_B}{W} \right)^2 \right] \quad \{23\}$$

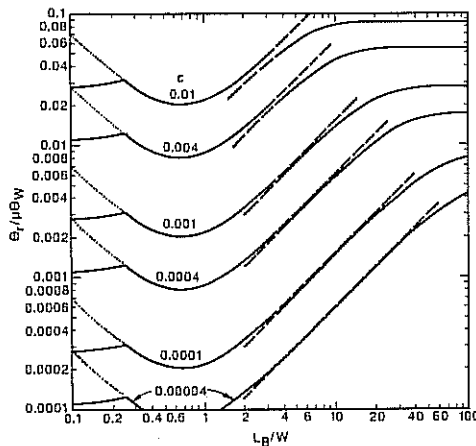


Figure 23 – Prevention of Interaction With Wrap of Roller
E / G = 2.7 (short spans)

for $(L_B/W) < 0.25$. Note that strain, not a variable in inequalities {6} and {8}, has now become an independent variable in inequalities {21} and {23}; furthermore, strain is a component (along with L_B/W) of KL_B in inequality {22}.

Inequalities {21}, {22}, and {23} are plotted in Figure 23, where any value below the appropriate curve is acceptable for prevention of interaction. Figure 23 is based on the commonly acceptable value of E/G of 2.7. The minima in Figure 23 occur at a value of L_B/W of 0.671, where $\theta_r / \mu\theta_w$ is approximately equal to 2ε (if $E/G = 2.7$):

$$\frac{\theta_r}{\mu\theta_w} < 2.01 \varepsilon \quad \{24\}$$

Figure 23 shows that the simple equation {24} is a reasonably accurate guideline for prevention of interaction of a span and its upstream neighbor for any span with a L/W ratio of approximately 2.0 or less. Equation {24} might be used as a conservative specification for *all* similar rollers on a process machine after the determination of μ at the operating speed, or the increase of μ to an acceptable level.

Note that θ_r applies to a downstream roller, while μ and θ_w (or f in previous analyses) apply to the next upstream roller (between potentially interacting spans). If interaction of several similar spans is to be prevented, the specification of equation {24} should be cut in half, because of the possibility of misalignment of successive rollers in opposite directions. The alignment criterion for prevention of interaction then becomes

$$\theta_r < \mu\theta_w\varepsilon. \quad \{25\}$$

For 90 degrees of wrap the criterion is $\theta_r < 1.5\mu\varepsilon$, or for 180 degrees of wrap it is $\theta_r < 3.1\mu\varepsilon$. If the rollers of a bridle as in Figure 4 are located with great precision relative to each other and if the span between them is very short, θ_w can be considered the sum of the wraps, perhaps about 8.0 radians for two rollers.

Inequality {24} provides a persuasive argument for misalignment as the cause of the severe lateral handling problems in the steel industry – the usual low value of strain dictates extreme accuracy of alignment, especially for the common long spans, yet accumulators lack the stiffness needed for precise alignment.

Increasing the coefficient of friction may be a practical method of avoiding interaction of spans. Good [4] related roughness of the web and roller to the interfacial friction, allowing predictable friction with rollers of a given roughness as achieved by plasma coating, grooving, or other methods.

CONCLUSIONS

For analysis of the interaction of two spans because of a misaligned downstream roller, a short span can be defined as a span having L/W less than 3.5, and a long span as one having L/W greater than 3.5.

Analysis of a uniform load on a slipping roller can be successfully applied to a wrapped roller with a nonuniformity of loading as great as the triangular load distribution caused by borderline slackness of an edge.

A steering guide should not be installed in a location with an entering span shorter than the pre-entering span unless friction and wrap on the roller between the spans are great enough at operating speeds to prevent the upstream transfer of moment, or unless a suitable nip roller or vacuum roller prevents the transfer of moment.

A fixed roller with a short entering span relative to its pre-entering span should be aligned very precisely, or precautions should be taken to prevent the upstream transfer of moment across the roller between the two spans; otherwise, erratic lateral errors will result as the coefficient of friction changes.

The pre-entering span may become an effective extension of the entering span as $\theta_r Et / f\mu$ becomes large in rare guiding applications.

REFERENCES

1. Shelton, J. J., Lateral Dynamics of a Moving Web. Ph.D. Thesis, Oklahoma State University, Stillwater, Oklahoma (July, 1968).
2. Shelton, J. J., "An Initially Straight Moving Web with a Slack Edge: Steady State Behavior Caused by Roller Nonparallelism Greater than Critical." Web Handling – 1992. The Applied Mechanics Division, ASME. (The Winter Annual Meeting of the American Society of Mechanical Engineers, Anaheim, California, Nov. 8–13, 1992).
3. Shelton, J. J., "A Simplified Model for Lateral Behavior of Short Web Spans," Proceedings of the Sixth International Conference on Web Handling, Oklahoma State University, Stillwater, Oklahoma, pp. 469-484, 2001.
4. Good, J. K., "Shear in Multispan Web Systems," Proceedings of the Fourth International Conference on Web Handling, Oklahoma State University, Stillwater, Oklahoma, pp. 264-286, 1997.

Name & Affiliation

Tim Walker
TJWalker & Associates

Question

What happens to the web when the central roller allows tension variations to cross over? You are looking at a two-span, three-roller setup and you have a misaligned downstream (setup) roller. For small misalignments at the downstream roller the traction between the central roller and the web may be sufficient to isolate the upstream span. There will be some level of misalignment at the downstream roller that will cause slippage between the web and the middle roller.

Name & Affiliation

John Shelton
Oklahoma State University

Answer

If this is a web guide, it would guide fine for a very small errors. You would have the same amount of error feeding into the entering span as you have feeding into the pre-entering span until it starts slipping. But when it starts trying to correct more error, the web goes farther in the direction of the original error. The error is amplified by the interaction of spans.

Name & Affiliation

Tim Walker
TJWalker & Associates

Comment

So if the friction was infinite on the middle roller, we are really saying there is no motion in the pre-entering span. Then when the friction on the middle roller drops to a point, the tension crosses over and we see a new position at which the web wants to run. That is what you are calling a jump.

Name & Affiliation

John Shelton
Oklahoma State University

Answer

Yes. The jump I am talking about only occurs for some L/W ratios where the web was running at one position and we have a small upstream error. Before it starts slipping, interacting, you have the same error at the entering roller as you have at the pre-entering roller. When the friction decreases enough that you have interaction, then you have a completely different operating point at the entering roller than you had previously. Usually, you have a smooth transition between the nonslipping condition and the slipping condition, but sometimes it moves a finite distance, 1 inch maybe, in a few seconds. This is what I am saying that some people have attributed to camber. You don't measure camber or friction online, so you guess at what may be causing this change in lateral position. I am saying that it is probably quite often interacting spans and not camber or something else that is causing this change of lateral position.

Name & Affiliation
Tim Walker
TJWalker & Associates

Question
The magnitude of misalignment is fairly typical of things you would find in a reasonably aligned machine. Do you also expect this would cause weave in wound rolls?

Name & Affiliation
John Shelton
Oklahoma State University

Question
Alignment of winding rolls – is that your question?

Name & Affiliation
Tim Walker
TJWalker & Associates

Answer
Either that or an aberration in a wound roll.

Name & Affiliation
John Shelton
Oklahoma State University

Answer
You might have either a tapered winding roll that would cause interaction of spans. For prevention of interaction, alignment must improve as the frictional grip decreases, and as the modulus of elasticity and thickness of the web increase. Interaction can therefore occur in well-aligned machines if friction, wrap of rollers, and other variables raise the variable $\theta_r E t / f \mu$ higher than a certain magnitude.